# Semi-algebraic optimization of temperature compensation in a general switch-type negative feedback model of circadian clocks

**Sven Ole Aase · Peter Ruoff**

**Keywords:**
Circadian clocks
Negative feedback (Goodwin) oscillator
Temperature compensation
Sensitivity analysis
Lowpass filtering
Operator
Optimization

**Mathematics Subject Classification** 93E11 · 92C40 · 34A30

**Abstract** Temperature compensation is an essential property of circadian oscillators which enables them to act as physiological clocks. We have analyzed the temperature compensating behavior of a generalized transcriptional–translational negative feedback oscillator with a hard hysteretic switch and rate constants with an Arrhenius-type temperature dependence. These oscillations can be considered as the result of a lowpass filtering operator acting on a train of rectangular pulses. Such a signal-processing viewpoint makes it possible to express, in a semi-algebraic manner, the period length, the oscillator's control (sensitivity) coefficients, and the first and second-order derivatives of the period–temperature relationship. We have used the semi-algebraic approach to investigate a 3-dimensional Goodwin-type representation of the oscillator, where local optimization for temperature compensation has been considered. In the local optimization, activation energies are found, which lead to a zero first order derivative and to a closest-to-zero second order derivative at a given reference temperature. We find that the major contribution to temperature compensation over an extended temperature range is given by the (local) zero first order derivative, while only minor contributions to temperature compensation are given by an optimized second order derivative. In biological terms this could be interpreted to relate to a circadian clock mechanism which during evolution is being optimized for a certain but relative narrow (habitat) temperature range.

## 1 Introduction

Biological clocks are physiological oscillators which play an important role in the adaptation of organisms to their environments [3,6,7]. Among the most intensively studied biological clocks we have circadian oscillators which have a period length of approximately 24 h (the name is derived from latin *circa*, about and *dies*, day). Circadian rhythms adapt (entrain) organisms to daily light/dark cycles, take part in the control of sleep/wake cycles, but also take part in the control of annual events such as migration of birds, butterflies, flower induction, hibernation and reproduction [3,6,7]. Circadian rhythms are present in practically all eukaryotic species, ranging from single cell organisms to mammals and have been found even in cyanobacteria.

Circadian oscillators behave as true physiological clocks and possess the capability to keep their period length approximately constant against environmental fluctuations such as variations in temperature, pH, or nutrition [19,22]. Temperature compensation, i.e., the approximate constancy of the period within a certain, for the organism important physiological temperature range, is probably one of the best studied examples of period homeostasis in circadian rhythms [3,6,7].

Experiments with mutant organisms have shown that most of the circadian "pacemakers" consist of transcriptional–translational negative feedback loops [4]. Model studies have shown that circadian clock properties, including temperature compensation, can be simulated by negative feedback oscillators such as the Goodwin oscillator [10,11,25].

By considering a general reaction kinetic oscillator which consists of $N$ component processes, a condition for temperature compensation can be formulated [21,23]:

$$\frac{\mathrm{d}\ln P}{\mathrm{d}T} = \frac{1}{RT^2}\sum_{i=1}^{N} C_i^P \cdot E_i = 0, \tag{1}$$

where $P$ is the oscillator's period, the $C_i^P$'s are control (sensitivity) coefficients [8,14] (defined as $\partial \ln P/\partial \ln k_i$) and $E_i$, $R$, and $T$ are the activation energies for each component process, the gas constant and the temperature (in Kelvin), respectively. In case the period P is a homogeneous function [1] of the rate constants ki , the control coefficients obey the summation theorem [8,14]:

$$\sum_{i=1}^{N} C_i^P = -1. \tag{2}$$

However, Eq. 1 is only valid for a given reference temperature $T_{\mathrm{ref}}$ for which the temperature-dependent $C_i^P$'s are calculated. This means that the condition of Eq. 1

cannot guarantee that temperature compensation will occur over an extended temper-ature interval around $T_{\mathrm{ref}}$. Because temperature compensation is considered in this paper with respect to a given reference point ($T_{\mathrm{ref}}$), the optimization procedure occurs locally at $T_{\mathrm{ref}}$, where the second-order derivative of the period with respect to temperature is also used for optimization. Furthermore, we develop a novel semi-algebraic approach in order to find the period, and its derivatives. The model we use is a generalized switch-type transcriptional–translational negative feedback oscillator, for which a 3-dimensional version has successfully been used to describe different properties of the *Neurospora* circadian clock [23].

## 2 Methods of calculation

System analysis using symbolic and numerical calculations was performed with the use of MATLAB (ver. 7.0.4, The Mathworks, Natick, MA, USA). Some simulation calculations were performed using the open access FORTRAN subroutine LSODE [20]. In comparison, MATLAB and LSODE gave essentially identical results.

## 3 A theory for semi-algebraic analysis

In this work we analyse a set of coupled differential equations of the following form:

$$\begin{aligned}
\dot{x}_1 &= k_1 f(x_n) - k_{n+1} x_1 \\
\dot{x}_2 &= k_2 x_1 - (k_3 + k_{n+2}) x_2 \\
\dot{x}_3 &= k_3 x_2 - (k_4 + k_{n+3}) x_3 \\
&\vdots \\
\dot{x}_i &= k_i x_{i-1} - (k_{i+1} + k_{n+i}) x_i \\
&\vdots \\
\dot{x}_{n-1} &= k_{n-1} x_{n-2} - (k_n + k_{2n-1}) x_{n-1} \\
\dot{x}_n &= k_n x_{n-1} - k_{2n} x_n
\end{aligned} \tag{3}$$

where $x_1, \ldots, x_n$ is a vector of $n$ system variables describing concentrations of intermediates $X_1, \ldots, X_n$, and where $k_1, \ldots, k_{2n}$ are rate constants. The equations define a transcriptional translational negative feedback oscillator shown in Fig. 1. The oscillations are driven by the "switch" term $f(x_n)$ which can only take two values, 0 and 1. As indicated in Fig. 2, $f$ can be a step function, or a hysteresis. In the case of hysteresis, the transcriptional on/off occurs at different $x_n$ values.

In general, there are no analytical methods for solving systems such as given in Eq. 3. The aim of our study was to find expressions for the period of the circadian clock, $P$, as well as gaining insight on how $P$ is influenced by the rate constants $k_1, \ldots, k_{2n}$. Due to reaction kinetic constraints the $x_i$ and $k_i$ parameters are real positive numbers.

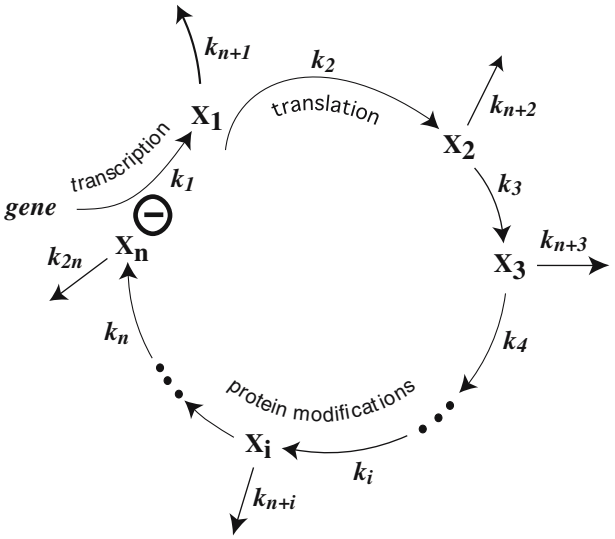


**Fig. 1** General transcriptional–translational negative feedback model (Eqs. 3) for circadian rhythms. Transcription and translation are the processes of making mRNA ($X_1$) and clock protein ($X_2$), respectively. The modification reactions are processes which can lead to clock protein species $X_i$ with altered properties, for example stability [5]

### 3.1 Linear system analysis

Using standard linear algebra notation, the system in Eq. 3 can be written as

$$\underbrace{\begin{bmatrix} \dot{x}_1 \\ \dot{x}_2 \\ \dot{x}_3 \\ \vdots \\ \dot{x}_{n-1} \\ \dot{x}_n \end{bmatrix}}_{\dot{\mathbf{x}}} = \underbrace{\begin{bmatrix} -k_{n+1} & 0 & & \cdots & 0 \\ k_2 & -(k_3+k_{n+2}) & 0 & & \\ 0 & & & & \vdots \\ \vdots & \ddots & \ddots & \ddots & \\ & & k_{n-1} & -(k_n+k_{2n-1}) & 0 \\ 0 & \cdots & 0 & k_n & -k_{2n} \end{bmatrix}}_{\mathbf{A}} \begin{bmatrix} x_1 \\ x_2 \\ x_3 \\ \vdots \\ x_{n-1} \\ x_n \end{bmatrix}_{\mathbf{x}} + \underbrace{\begin{bmatrix} k_1 f(x_n) \\ 0 \\ 0 \\ \vdots \\ 0 \\ 0 \end{bmatrix}}_{\mathbf{F}(x_n)} \tag{4}$$

where $\mathbf{x}$ is the vector of system variables, $\mathbf{A}$ is an $n \times n$ matrix of real constants, and $\mathbf{F}(x_n)$ contains the switch term $k_1 f(x_n)$. In the following analysis we interpret

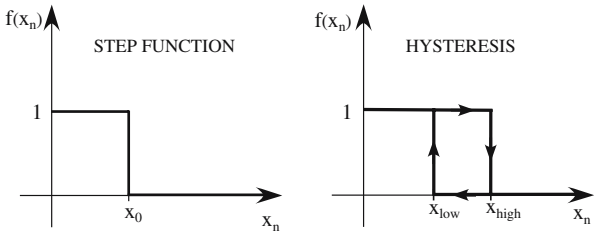


**Fig. 2** Switch types for controlling negative feedback

the second term in Eq. 4 as an *input signal* to the linear system characterized by the matrix **A**. The system variable $x_n(t)$ is considered as an *output signal*. Also note that due to the special structure of Eq. 3, **A** is a band-matrix: Only elements on the diagonal and the first lower sub-diagonal are nonzero. It follows that the eigenvalues of the **A** matrix are given as

$$\begin{aligned}\lambda_1 &= -k_{n+1}\\ \lambda_2 &= -(k_3 + k_{n+2})\\ &\vdots\\ \lambda_{n-1} &= -(k_n + k_{2n-1})\\ \lambda_n &= -k_{2n}.\end{aligned} \tag{5}$$

A standard tool for analysing coupled, linear differential equations is the Laplace transformation. Eq. 3 is transformed to

$$\begin{aligned}sX_1(s) &= k_1 F(s) + \lambda_1 X_1(s)\\ sX_i(s) &= k_i X_{i-1}(s) + \lambda_i X_i(s), \quad i = 2, \ldots, n.\end{aligned} \tag{6}$$

where we have temporarily ignored the $x_n$-dependence of $F(s)$. By straightforward algebraic manipulation we can now find the input–output relation defined as

$$H(s) = \frac{X_n(s)}{F(s)} = \frac{X_n(s)}{X_{n-1}(s)}\frac{X_{n-1}(s)}{X_{n-2}(s)}\cdots\frac{X_2(s)}{X_1(s)}\frac{X_1(s)}{F(s)} = \prod_{i=1}^{n}\frac{k_i}{s-\lambda_i}. \tag{7}$$

The poles in Eq. 7 are identical to the eigenvalues of **A** and characterize the linear part of the differential equation system. Assuming distinct eigenvalues the inverse Laplace transform can be found using partial fracture decomposition, and gives the causal time-domain input–output relation:[1]

$$h(t) = \begin{cases} \sum_{i=1}^{n} K_i e^{\lambda_i t}, & t \geq 0,\\ 0, & t < 0,\end{cases} \quad \text{where} \tag{8}$$

[1] This is commonly referred to as the *unit pulse response* in electrical engineering literature.

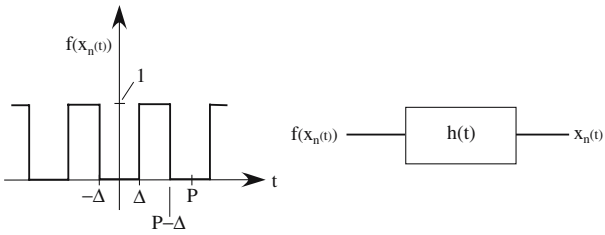


**Fig. 3** System interpreted as a filtering operator

$$K_i = \left( \prod_{j=1}^{n} k_j \right) \prod_{\substack{j=1 \\ j \neq i}}^{n} \frac{1}{\lambda_i - \lambda_j}. \tag{9}$$

Due to the rate constants $k_1, \ldots, k_{2n}$ all being real and positive, the eigenvalues are real and negative, so the input–output relation of Eqs. 7 and 8 constitutes a *lowpass filter.*

### 3.2 Nonlinear feedback analysis

For the purpose of analysing the period $P$ of the system, we make the following assumptions:

1. The rate constants are chosen such that the system oscillates. Furthermore, we assume that the system has reached the limit-cycle. All state variables are therefore periodic signals, i.e., $x_i(t + P) = x_i(t)$.
2. During one period, the "switch" term $f(x_n(t))$ undergoes exactly 2 transitions, reflecting the "on/off" behavior of the gene's transcriptional activity. The use of a hysteretic switch as shown on the right panel of Fig. 2 was inspired by observing similar behavior (i.e., observation of different excitation thresholds between oxidized and reduced states) in a model of a chemical oscillator [24].

With the assumptions above we can model the system as a lowpass filtering operator working on an infinite sequence of rectangular pulses. This is illustrated in Fig. 3. The filter output is the system variable $x_n(t)$. Since we have a lowpass filter, the behavior of $x_n(t)$ will be more slowly varying compared to the input pulse signal, as well as being continuous. In order for the model to correspond directly with the original differential equations, the value of $x_n$ must match the threshold value at the associated switch-points. Logically, the limit-cycle assumption stated above dictates the behavior of the switch variable $x_n$ as shown in Table 1 (see Fig. 2).

With reference to Figs. 2 and 3, we can fix the values of the output signal at switching times $\Delta$ and $P$ as follows:

$$\text{Step function: } x_n(\Delta) = x_n(P - \Delta) = x_0 \tag{10}$$

$$\text{Hysteresis: } x_n(\Delta) = x_{\text{low}} \tag{11}$$

$$x_n(P - \Delta) = x_{\text{high}}. \tag{12}$$

**Table 1** Variable transition table showing the next transition, given the current state and the switch type

| | Current state | |
|---|---|---|
| Switch type | $f = 1$ | $f = 0$ |
| Step function | $x_n \to x_0^-$ | $x_n \to x_0^+$ |
| Hysteresis | $x_n \to x_{\text{high}}^-$ | $x_n \to x_{\text{low}}^+$ |

Using the lowpass filter viewpoint, the output signal at switch-time $t = \Delta$ is found as the convolution between an infinite sequence of rectangular pulses $f(x_n(t))$, and the unit pulse response $h(t)$:

$$\begin{aligned} x_n(\Delta) = (h * f)(\Delta) &= \int_0^\infty h(\tau) f(\Delta - \tau) d\tau, \\ &= \sum_{k=1}^{\infty} \int_{2\Delta+(k-1)P}^{kP} h(\tau) d\tau = \sum_{k=1}^{\infty} \sum_{i=1}^{n} \int_{2\Delta+(k-1)P}^{kP} K_i e^{\lambda_i \tau} d\tau \\ &= \sum_{i=1}^{n} \frac{K_i}{\lambda_i} \sum_{k=1}^{\infty} (e^{\lambda_i kP} - e^{\lambda_i (2\Delta+(k-1)P)}) \\ &= \sum_{i=1}^{n} \frac{K_i}{\lambda_i} \left( e^{\lambda_i P} \frac{1}{1 - e^{\lambda_i P}} - e^{2\lambda_i \Delta} \frac{1}{1 - e^{\lambda_i P}} \right) \\ &= \sum_{i=1}^{n} \frac{K_i}{\lambda_i} \frac{e^{\lambda_i P} - e^{2\lambda_i \Delta}}{1 - e^{\lambda_i P}}. \end{aligned} \tag{13}$$

Similarly, the expression for the output variable at switch-time $t = P - \Delta$ is found to be

$$x_n(P - \Delta) = \sum_{i=1}^{n} \frac{K_i}{\lambda_i} \frac{e^{\lambda_i (P-2\Delta)} - 1}{1 - e^{\lambda_i P}}. \tag{14}$$

For the hysteresis case[2], we set

$$G_1 \stackrel{\Delta}{=} x_n(\Delta) - x_{\text{low}} = 0 \tag{15}$$

$$G_2 \stackrel{\Delta}{=} x_n(P - \Delta) - x_{\text{high}} = 0, \tag{16}$$

giving two equations with the unknowns $P$ and $\Delta$. Since the solution of our differential equation, if it exists, is unique[3], this only produces one solution for $(P, \Delta)$.

[2] Replace $x_{\text{low}}$ and $x_{\text{high}}$ with $x_0$ in the step function case.

[3] Strictly speaking, the uniqueness of the solution is generally guaranteed only for systems where the components have continuous first order derivatives. Since our system contains a step function, this is violated. However, interpreting the system as a lowpass filter applied to rectangular pulses, we can obtain an arbitrarily good system approximation using pulses with smooth transitions.

Unfortunately, Eqs. 15 and 16 does not give a solution which is algebraically simple, and in practice a numerical solution for $(P, \Delta)$ has to be found. An illustration of this will be shown in Sect. 5.

### 3.3 Computing derivatives

For analysing temperature compensation we want to compute the following entities algebraically:

$$\frac{\partial \ln P}{\partial \ln k_i}, \quad \frac{\partial^2 \ln P}{\partial \ln k_i \partial \ln k_j}, \quad i, j = 1, \ldots, n. \tag{17}$$

Although not explicitly solvable for $P$, we can still use Eqs. 15 and 16 to find derivatives in a semi-algebraic manner. Noting that $G_m = G_m(\ln k_1, \ldots, \ln k_{2n}, P, \Delta)$, $m = 1, 2$, where $P = P(\ln k_1, \ldots, \ln k_{2n})$ and $\Delta = \Delta(\ln k_1, \ldots, \ln k_{2n})$, we can differentiate $G_m$ with respect to $\ln k_i$ using the generalized chain rule:

$$\frac{\partial G_m}{\partial \ln k_i} + \frac{\partial G_m}{\partial \ln P}\frac{\partial \ln P}{\partial \ln k_i} + \frac{\partial G_m}{\partial \ln \Delta}\frac{\partial \ln \Delta}{\partial \ln k_i} = 0, \quad m = 1, 2. \tag{18}$$

These are linear equations in the unknowns $\frac{\partial \ln P}{\partial \ln k_i}$ and $\frac{\partial \ln \Delta}{\partial \ln k_i}$ and we can find the desired unknown as

$$\frac{\partial \ln P}{\partial \ln k_i} = \frac{\frac{\partial G_1}{\partial \ln \Delta}\frac{\partial G_2}{\partial \ln k_i} - \frac{\partial G_1}{\partial \ln k_i}\frac{\partial G_2}{\partial \ln \Delta}}{\frac{\partial G_1}{\partial \ln P}\frac{\partial G_2}{\partial \ln \Delta} - \frac{\partial G_1}{\partial \ln \Delta}\frac{\partial G_2}{\partial \ln P}}, \quad i = 1, \ldots, 2n. \tag{19}$$

Similarly, a straightforward, but tedious derivation leads to the following expression for the second derivatives:

$$\frac{\partial^2 \ln P}{\partial \ln k_i \partial \ln k_j} = \frac{\frac{\partial G_1}{\partial \ln \Delta}A_{ij}^{(2)} - A_{ij}^{(1)}\frac{\partial G_2}{\partial \ln \Delta}}{\frac{\partial G_1}{\partial \ln P}\frac{\partial G_2}{\partial \ln \Delta} - \frac{\partial G_1}{\partial \ln \Delta}\frac{\partial G_2}{\partial \ln P}}, \tag{20}$$

where

$$\begin{aligned} A_{ij}^{(m)} = {} & \frac{\partial^2 G_m}{\partial \ln k_i \partial \ln k_j} + \frac{\partial^2 G_m}{\partial \ln k_i \partial \ln P}\frac{\partial \ln P}{\partial \ln k_j} + \frac{\partial^2 G_m}{\partial \ln k_i \partial \ln \Delta}\frac{\partial \ln \Delta}{\partial \ln k_j} \\ & + \left(\frac{\partial^2 G_m}{\partial \ln k_j \partial \ln P} + \frac{\partial^2 G_m}{\partial^2 \ln P}\frac{\partial \ln P}{\partial \ln k_j} + \frac{\partial^2 G_m}{\partial \ln P \partial \ln \Delta}\frac{\partial \ln \Delta}{\partial \ln k_j}\right)\frac{\partial \ln P}{\partial \ln k_i} \\ & + \left(\frac{\partial^2 G_m}{\partial \ln k_i \partial \ln \Delta} + \frac{\partial^2 G_m}{\partial \ln P \partial \ln \Delta}\frac{\partial \ln P}{\partial \ln k_j} + \frac{\partial^2 G_m}{\partial^2 \ln \Delta}\frac{\partial \ln \Delta}{\partial \ln k_j}\right)\frac{\partial \ln \Delta}{\partial \ln k_i}, \\ & m = 1, 2, \quad i, j = 1, \ldots, 2n. \end{aligned} \tag{21}$$

Given the rate constants $k_1, \ldots, k_{2n}$, we can solve for $(P, \Delta)$ numerically using Eqs. 15 and 16 and then find the first and second order derivatives from Eqs. 19, 20, and 21.

## 4 Local curve optimization for temperature compensation

A change in temperature from, say $T_{min}$ to $T_{max}$ will, according to the Arrhenius equation

$$k_i = A_i e^{-\frac{E_i}{RT}} \tag{22}$$

define a parametric curve in $R^{2n}$, the Euclidian space spanned by the $2n$ reactions/rate constants.

In order to achieve temperature compensation, temperature-induced changes in each $k_i$ need to cancel out any changes in the system period $P$. In this section we provide a local theory for optimal temperature compensation: Given initial $k_1^{\text{ref}}, \ldots, k_{2n}^{\text{ref}}$ and an associated initial temperature $T_{\text{ref}}$, the task is to find the optimal set of activation energies $E_1, \ldots, E_{2n}$ such that the period will be affected as little as possible when the temperature is changed within a certain temperature interval. The criterion for optimization is that the first order derivative of the period with respect to temperature is zero and that the second order derivative is at a minimum.

Starting with the first order derivative, we can write [23]:

$$\left.\frac{\partial \ln P}{\partial T}\right|_{T=T_{\text{ref}}} = \sum_{i=1}^{2n} \frac{\partial \ln P}{\partial \ln k_i} \frac{\partial \ln k_i}{\partial T} = \frac{1}{RT^2} \sum_{i=1}^{2n} \frac{\partial \ln P}{\partial \ln k_i} E_i. \tag{23}$$

It follows that the inner product of the activation energies and the control coefficients $C_i^P = \frac{\partial \ln P}{\partial \ln k_i}$ vanishes.

The second derivative is found as:

$$\begin{aligned}\left.\frac{\partial^2 \ln P}{\partial^2 T}\right|_{T=T_{\text{ref}}} &= -\frac{2}{RT^3} \underbrace{\sum_{i=1}^{2n} \frac{\partial \ln P}{\partial \ln k_i} E_i}_{0} + \frac{1}{RT^2} \sum_{i=1}^{2n} \sum_{j=1}^{2n} \frac{\partial^2 \ln P}{\partial \ln k_j \partial \ln k_i} \underbrace{\frac{\partial \ln k_j}{\partial T}}_{\frac{E_j}{RT^2}} E_i \\ &= \frac{1}{R^2 T^4} \sum_{i=1}^{2n} \sum_{j=1}^{2n} \frac{\partial^2 \ln P}{\partial \ln k_j \partial \ln k_i} E_j E_i = \frac{1}{R^2 T^4} \mathbf{E^T H E},\end{aligned} \tag{24}$$

where $\mathbf{H}$ is the Hessian matrix of second derivatives and $\mathbf{E}$ is the vector of activation energies.

## 5 A Goodwin-type model with hysteretic switch

A 3-dimensional representation of Eq. 3 with a hysteretic switch has recently been studied numerically in connection with the *Neurospora* circadian clock [23].

**Table 2** Rate constants, control coefficients, and optimal activation energies at reference temperature $T_{\text{ref}} = 292$ K

| Reaction $i$ | Rate constant $k_i, h^{-1}$ | Control coefficient $C_i^P$ | Optimal activation energy $E_i$, kJ/mol |
|---|---|---|---|
| 1 | 0.30 | 0.100 | 200.0 |
| 2 | 0.30 | 0.100 | 159.3 |
| 3 | 0.30 | −0.096 | 30.0 |
| 4 | 0.27 | −0.455 | 30.0 |
| 5 | 0.20 | −0.131 | 30.0 |
| 6 | 0.20 | −0.518 | 30.0 |

In *Neurospora* the circadian pacemaker is closely related to the expression of the *frequency* (*frq*) gene into its protein (FRQ), which is regulated by a negative feedback, i.e., expressed FRQ protein inhibits its own transcription [2,5]. In a 3-dimensional representation of the model (Fig. 1), $x_1$ corresponds to *frq*-mRNA concentration, $x_2$ to the cytosolic concentration of FRQ ($\text{FRQ}_c$), and $x_3$ to its nuclear concentration of FRQ ($\text{FRQ}_n$).

Table 2 shows the rate constant values defined at $T_{\text{ref}} = 19$ °C (292 K) [23] together with the control coefficients (Eq. 19) calculated semi-algebraically at $T_{\text{ref}}$. These rate constants refer to the *wild-type* strain ($frq^+$) for which FRQ degradation rate constants (and activation energies) have been experimentally estimated [23]. The hys-teretic switch is defined as follows: when the nuclear FRQ concentration ($x_3$) exceeds an upper threshold, $x_3 \geq x_{\text{high}} = 0.1$ a.u., $f(x_3)$ is set to zero, which leads to a stop in transcription and to a decrease of *frq*-mRNA ($x_1$), $\text{FRQ}_c$ ($x_2$), and $\text{FRQ}_n$ ($x_3$), because of the degradation reactions corresponding to the rate constants $k_4$, $k_5$, and $k_6$. Transcription is started again when the (decreasing) $x_3$ has reached a lower threshold ($\leq x_{\text{low}} = 0.05$ a.u.) [23].

Figure 4 shows the implicitly defined functions $G_1(P, \Delta) = 0$ and $G_2(P, \Delta) = 0$ for the system defined in Table 2. The unique solution for $(P, \Delta)$ is found numerically as the intersection of the two curves.

### 5.1 Local curve optimizations

Starting with the set of rate constants in Table 2 (defined at $T_{\text{ref}}$), we determine a locally optimized set of activation energies, i.e., finding those $E_i$'s, which makes Eq. 23 zero, while keeping the second derivative (Eq. 24) as close to zero as possible. This was done in Matlab using the quadratic programming command *quadprog*. As in a previous study [23] the activation energies were limited to the 30–200 kJ/mol range. As can be seen from Table 2, the optimal choice of activation energies is found by choosing values on the grid limit, except for $E_2 = 159.3$ kJ/mol.

The solid line in Fig. 5 shows the period as a function of temperature using the optimized activation energies for $T_{\text{ref}} = 292$ K. In addition, 100 period–temperature relationships are shown as dotted lines when activation energies were randomly selected from a uniform distribution between 30 and 200 kJ/mol. The figure

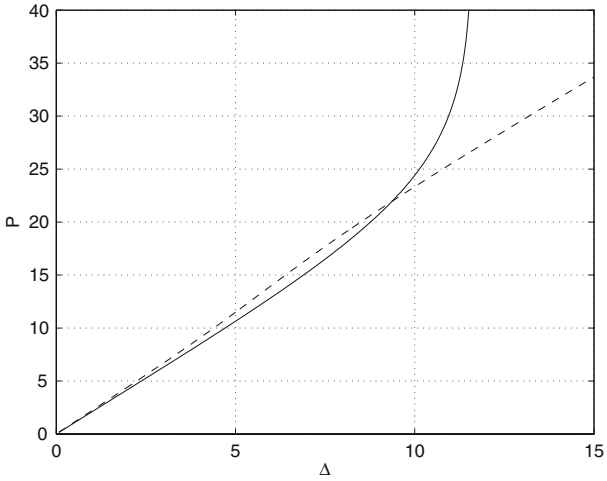


**Fig. 4** Solving for $(P, \Delta)$ using Eqs. 15 and 16. $G_1$ is plotted as a *solid line*, $G_2$ is plotted as a *dotted line*

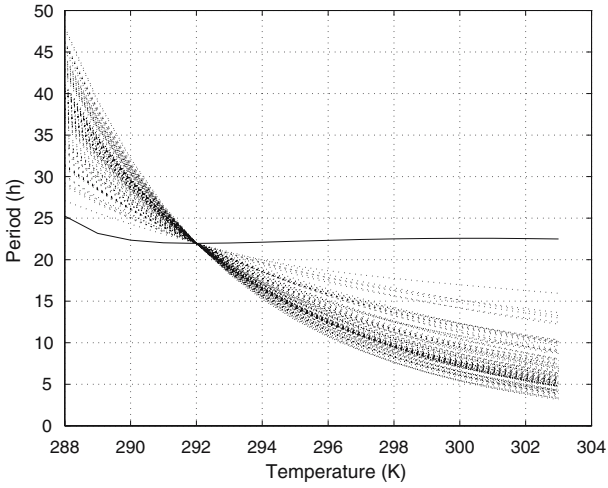


**Fig. 5** Temperature–period curve for locally optimized activation energies (*solid line*). This is contrasted with nonoptimized curves (*dotted lines*) when randomly selected activation energies in the allowed energy range are used. By definition, all curves intersect at the reference temperature $T_{\text{ref}} = 292$ K

clearly reveals the significance of having a well chosen set of activation energies for temperature compensation.

The locally optimized curve in Fig. 5 is found using criteria for the first and second order derivatives. A more simplified optimization can be done using the first order derivatives only. This allows for many solutions for the activation energies since the equations

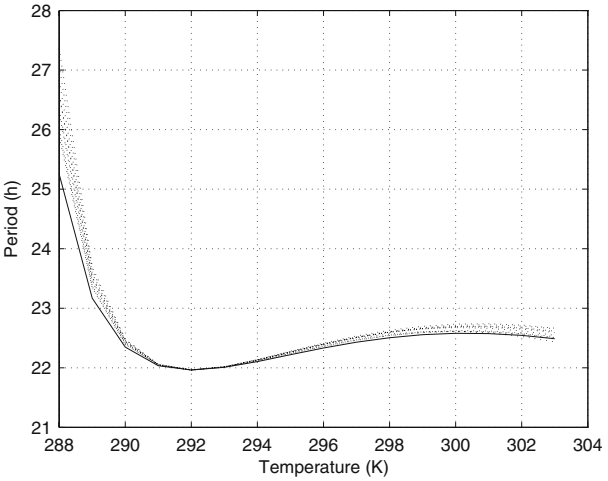


**Fig. 6** *Solid line* shows the optimized curve of Fig. 5 for vanishing first order and minimized second order derivatives. In comparison, the *dotted lines* show curves where only the first order derivative (Eq. 1) is zero without a minimized second order derivative

$$\sum_{i=1}^{6} C_i^P E_i = 0, \tag{25}$$

$$30 \leq E_i \leq 200\ , \quad i = 1, \ldots, 6. \tag{26}$$

define the solution set as the intersection between a 5-dimensional space (defined by Eq. 25) and a 6 dimensional hypercube (defined by Eq. 26). Figure 6 shows the obtained results when using activation energies randomly selected within this solution set. A procedure for finding such solutions is to project the uniformly distributed E-vectors used in Fig. 5 onto the 5-dimensional space and then remove solution not satisfying Eq. 26. Figure 6 compares the temperature-period curves obtained in this fashion with the curve obtained when additionally minimizing the second order derivative.

Although the model's temperature compensation is generally in good agreement with experimental results [23], it is not able to show the experimentally observed over-compensation (i.e., the period increases with increasing temperature) [9] at the lower end of *Neurospora's* temperature range (Fig. 5). We believe that this is related to the relative simple structure of the model.

## 6 Discussion

Temperature compensation is one of the defining and canonical properties of circadian rhythms [3,7]. Although molecular and theoretical explanations for many aspects of circadian oscillators have been developed over the past decade [6], there have been few attempts to describe temperature compensation on a mathematical kinetic basis [26]. For an overview on other or related attempts to explain temperature compensation the

reader is referred to the following papers [12,13,15–18,27,28]. However, a discussion of these various approaches on how to "balance P" is beyond the scope of this paper.

In many organisms the circadian pacemaker has been found to contain a transcriptional–translational negative feedback loop as described in Fig. 1. Transcription and translation of clock proteins as well as clock protein modifications are composed of many individual reactions and the usage of single rate constants and activation energies to each of the processes in Fig. 1 represent therefore a considerable simplification. Nevertheless, the transcriptional–translational negative feedback oscillator has been shown to describe many circadian clock properties [25,23].

Equation 1 was derived [21,23] by assuming an Arrhenius-type dependence between rate constants of the various component processes and temperature (Eq. 22), which is valid for all (elementary) chemical processes. In order to satisfy the condition for temperature compensation (Eq. 1), at least one of the control coefficients needs to be positive in order to "balance" the otherwise negative contributions (see Eq. 2). In the generalized model studied here, only transcription (synthesis of clock mRNA) and translation (synthesis of clock protein) show positive control coefficients (Table 2), indicating that the origin of temperature compensation is closely related to the processes involved in transcription and translation.

The algebraic methodology introduced in this article allows for better insight into this relationship. Inspection of the (lengthy) algebraic expressions for $G_1$ and $G_2$ (Eq. 15) reveals that in both expressions the $k_1$ and $k_2$ rate constants always appear as the product $k_1k_2$. It follows that the period must also depend on this product, i.e., $P = P(k_1k_2)$. Since $P$ is a homogenous function of $k_1$ and $k_2$ this implies that the associated control coefficients must be equal, $C_1^P = C_2^P$. From Eq. 1 we see that the first order derivative of the period–temperature relationship will be unaffected as long as the sum of $E_1$ and $E_2$ are kept constant.

The condition for temperature compensation (Eq. 1) is only valid for a given reference temperature ($T_{\text{ref}}$) at which rate constants are defined. This means that Eq. 1 does in principle not guarantee for temperature compensation beyond $T_{\text{ref}}$, i.e., over an extended temperature range. However, the results show that when comparing randomly selected activation energies with any activation energy combination satisfying Eq. 1, the system satisfying Eq. 1 (Fig. 5) leads to a much better temperature compensation, but not to a complete constancy of the period. Minimizing of the second-order derivative provides only a marginally improvement of temperature compensation (Fig. 6), indicating that higher-order derivatives contribute only little to the overall tempera-ture compensation. However, one has also to be careful when drawing more general conclusions from the study of a special model.

In conclusion, the local condition of temperature compensation given by Eq. 1 with constant activation energies provides most of the temperature compensation behavior in a general model for transcriptional–translational negative feedback oscillators. In biological terms this could be interpreted to relate to a circadian clock mechanism which during evolution is being optimized for a certain but relative narrow (habitat) temperature range.

**Acknowledgments** We thank Magnar Dale, Alexander Ulanovskii and Tormod Drengstig for helpful discussions.

## References


1. Apostol, T.M.: Calculus, vol II. Xerox College Publishing, Waltham (1969)
2. Aronson, B.D., Johnson, K.A., Loros, J.J., Dunlap, J.C.: Negative feedback defining a circadian clock: autoregulation of the clock gene frequency. Science **263**(5153), 1578–1584 (1994)
3. Bünning, E.: The Physiological Clock. Springer-Verlag, Berlin (1963)
4. Dunlap, J.C.: Molecular bases for circadian clocks. Cell **96**(2), 271–290 (1999)
5. Dunlap, J.C., Loros, J.J.: The Neurospora circadian system. J. Biol. Rhythms. **19**(5), 414–424 (2004)
6. Dunlap, J.C., Loros, J.J., DeCoursey, P.J. (eds.): Chronobiology. Biological Timekeeping. Sinauer Associates, Inc. Publishers, Sunderland (2004)
7. Edmunds, L.N.: Cellular and Molecular Bases of Biological Clocks. Springer-Verlag, New York (1988)
8. Fell, D.: Understanding the Control of Metabolism. Portland Press, London and Miami (1997)
9. Gardner, G.F., Feldman, J.F.: Temperature compensation of circadian periodicity in clock mutants of neurospora crassa. Plant Physiol. **68**, 1244–1248 (1981)
10. Goldbeter, A.: Computational approaches to cellular rhythms. Nature **420**(6912), 238–245 (2002)
11. Goodwin, B.C.: Oscillatory behavior in enzymatic control processes. Adv. Enzyme Regulat. **3**, 425–438 (1965)
12. Gould, P.D., Locke, J.C., Larue, C., Southern, M.M., Davis, S.J., Hanano, S., Moyle, R., Milich, R., Putterill, J., Millar, A.J., Hall, A.: The molecular basis of temperature compensation in the Arabidopsis circadian clock. Plant Cell **18**(5), 1177–1187 (2006)
13. Hastings, J.W., Sweeney, B.M.: On the mechanism of temperature independence in a biological clock. Proc. Natl. Acad. Sci. USA **43**, 804–811 (1957)
14. Heinrich, R., Schuster, S.: The Regulation of Cellular Systems. Chapman and Hall, New York (1996)
15. Hong, C.I., Conrad, E.D., Tyson, J.J.: A proposal for robust temperature compensation of circadian rhythms. Proc. Natl. Acad. Sci. USA **104**(4), 1195–1200 (2007)
16. Kurosawa, G., Iwasa, Y.: Temperature compensation in circadian clock models. J. Theor. Biol. **233**(4), 453–468 (2005)
17. Lakin-Thomas, P.L., Brody, S., Cote, G.G.: Amplitude model for the effects of mutations and temperature on period and phase resetting of the neurospora circadian oscillator. J. Biol. Rhythms **6**(4), 281–297 (1991)
18. Leloup, J.C., Goldbeter, A.: Temperature compensation of circadian rhythms: control of the period in a model for circadian oscillations of the per protein in Drosophila. Chronobiol. Int. **14**(5), 511–520 (1997)
19. Pittendrigh, C.S., Caldarola, P.C.: General homeostasis of the frequency of circadian oscillations. Proc. Natl. Acad. Sci. USA **70**(9), 2697–2701 (1973)
20. Radhakrishnan, K., Hindmarsh, A.C.: Description and use of LSODE, the Livermore Solver for Ordinary Differential Equations. Tech. Rep. NASA Reference Publication 1327, National Aeronautics and Space Administration, Lewis Research Center (1993)
21. Ruoff, P.: Introducing temperature-compensation in any reaction kinetic oscillator model. J. Interdiscipl. Cycle Res. **23**, 92–99 (1992)
22. Ruoff, P., Behzadi, A., Hauglid, M., Vinsjevik, M., Havås, H.: pH homeostasis of the circadian sporulation rhythm in clock mutants of Neurospora crassa. Chronobiol. Int. **17**(6), 733–750 (2000)
23. Ruoff, P., Loros, J.J., Dunlap, J.C.: The relationship between FRQ protein stability and temperature compensation in the Neurospora circadian clock. Proc. Natl. Acad. Sci. USA **102**(49), 17,681–17,686
24. Ruoff, P., Noyes, R.M.: Phase response behaviors of different oscillatory states in the Belousov–Zhabotinsky reaction. J. Chem. Phys. **89**, 6247–6254 (1988)
25. Ruoff, P., Rensing, L.: The temperature-compensated Goodwin model simulates many circadian clock properties. J. Theor. Biol. **179**, 275–285 (1996)
26. Ruoff, P., Vinsjevik, M., Rensing, L.: Temperature compensation in biological oscillators: A challenge for joint experimental and theoretical analysis. Comments Theor. Biol. **5**, 361–382 (2000)
27. Valeur, K.R., degli Agosti, R.: Simulations of temperature sensitivity of the peroxidase-oxidase oscillator. Biophys. Chem. **99**(3), 259–270 (2002)
28. Winfree, A.T.: The geometry of biological time, 2nd edn. Springer-Verlag, New York (2000)